FIRST-ORDER PHASE TRANSITIONS

WOLFHARD JANKE
Institut für Theoretische Physik, Universität Leipzig
Augustusplatz 10/11, D-04109 Leipzig, Germany

Abstract. The lecture starts with an overview of some of the most important properties of first-order phase transitions and their distinctive features compared with second-order transitions. Then special emphasis will be placed on the finite-size scaling behaviour of first-order phase transitions, which is essential for analyzing and interpreting numerical data obtained in computer simulations.

1. Overview

According to Ehrenfest's classification scheme, phase transitions may be classified as first-, second-, or higher-order transitions, depending on whether the first, second, or higher temperature derivative of the free energy becomes singular at the transition point [1]. Even though second-order phase transitions [2] and the associated critical phenomena have prompted a huge amount of experimental, theoretical and numerical activities over the last thirty years, the vast majority of phase transitions in nature is of first order [3, 4, 5, 6]. Examples cover many fields of physics and energy scales, ranging from simple and well studied phenomena such as field-driven transitions in magnets and temperature-driven melting of solid matter and various structural transitions in liquid crystals over the deconfining transition in hot quark-gluon matter to the much less understood transitions in the evolution of the early universe.

The most characteristic properties of first- and second-order phase transitions are sketched in Fig. 1. As is high-lighted there, the distinctive features of first-order phase transitions are phase coexistence and metastability, being reflected by jumps in the energy or magnetization and hysteresis effects upon heating or cooling the system or changing the magnetic field direction. At the transition temperature T_0 the correlation length ξ in the coexisting phases stays finite. This is in sharp contrast to a second-order phase transition where ξ diverges at the critical temperature T_c. The loss of an intrinsic length scale at T_c gives rise to critical phenomena and power-law singularities in thermodynamic functions governed by universal critical exponents α, β, γ, $\dots$ [2]. For first-order phase transitions, on the other hand, due to the finite correlation length no such universal power-law divergences can occur in response functions such as the specific heat C or magnetic susceptibility χ. Still, in large but finite systems, narrow peaks of C and χ are observed, which are remnants of the formal δ-function singularities emerging when differentiating the discontinuous energy and magnetization in the infinite-volume limit; cf. Fig. 1. Quite similar to a second-order phase transition, the location, width and height of these peaks scale in a characteristic way with the size of the system whose precise description is the subject of finite-size scaling (FSS) theory.

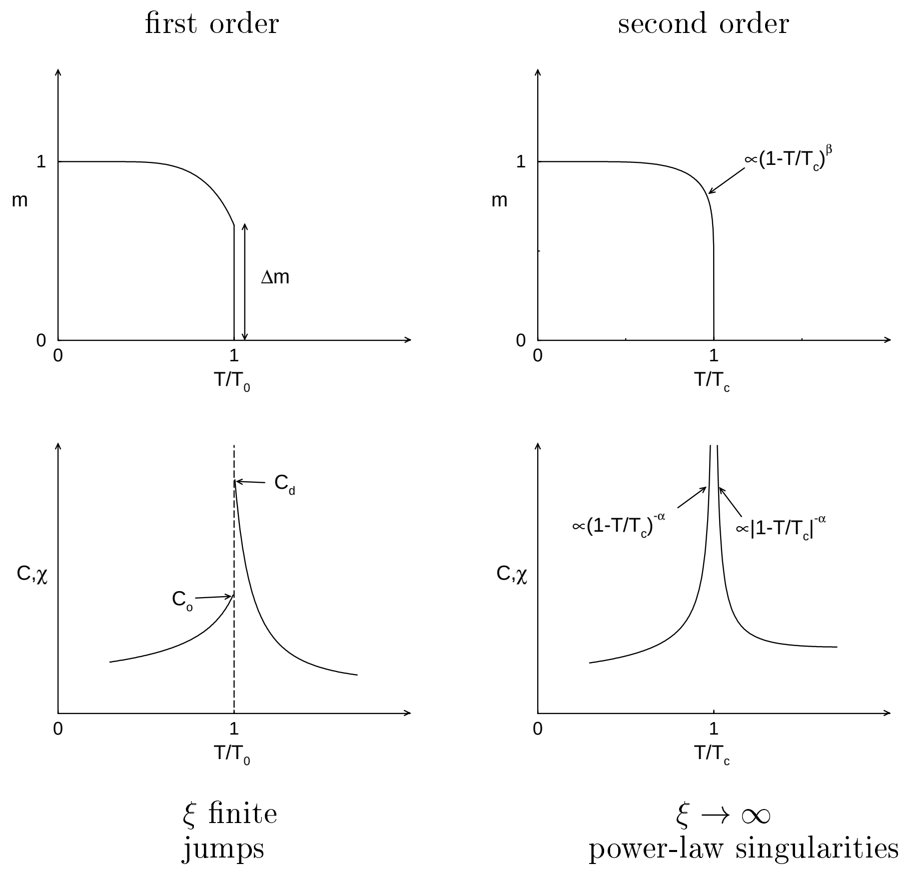

Figure 1. Sketch of the typical behaviour of the magnetization m, specific heat C, and susceptibility χ at first- and second-order phase transitions in the infinite-volume limit.

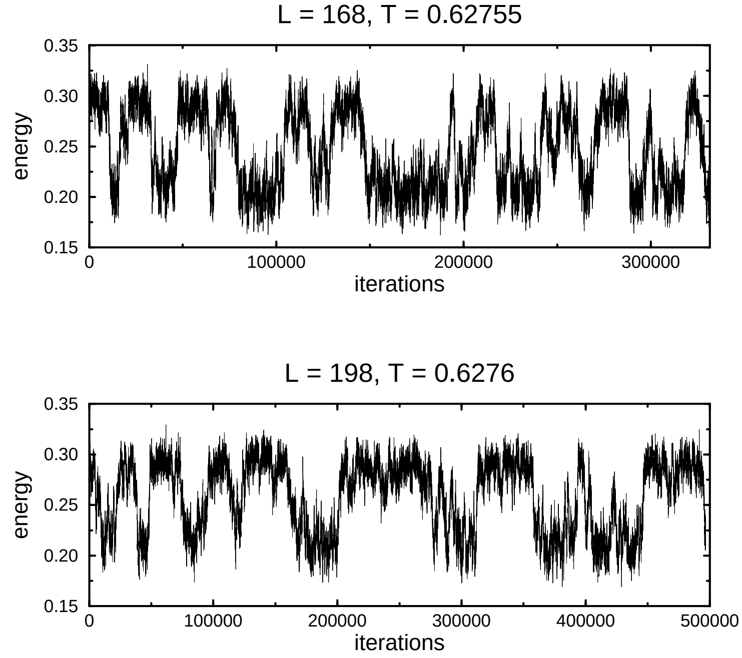

Figure 2. Energy time-series showing pronounced flips between the ordered and disordered phase. The data are taken from simulations of the three-state Potts antiferromagnetic model on a triangular lattice (3PAFT) [7], which exhibits a weak first-order phase transition.

When studying first-order phase transitions with Monte Carlo computer simulations it is straightforward to monitor the (pseudo-) time evolution of the system and to measure energy and magnetization densities. Close to T_0, metastability is reflected in the time evolution of a canonical simulation by flips between the two (or more) coexisting phases. For an illustration, taken from Monte Carlo simulations of the three-state Potts antiferromagnetic model on a triangular lattice (3PAFT) [7], see Fig. 2.

This gives rise to double-peaked energy or magnetization histograms, where the peaks represent the pure phases. A typical example is shown in Fig. 3. The dip between the two peaks is associated with the flips between the two phases which proceed via mixed phase configurations containing interfaces. If we apply periodic boundary conditions, there are for topological reasons always (at least) two interfaces costing additional energy parametrized by an interface tension σ. For a cubic system of size L^d this extra contribution to the free energy leads to a suppression of mixed phase configurations by an additional contribution to the Boltzmann factor $\propto \exp(-2\beta\sigma L^{d-1})$, where $\beta \propto 1/T$ is the inverse temperature, what

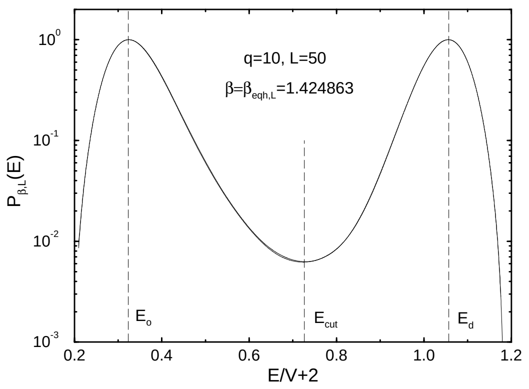

Figure 3. Canonical energy density of the 2D 10-state Potts model for a 50×50 lattice on a logarithmic scale reweighted to $\beta_{\mathrm{eqh},L}$ where the two peaks are of equal height.

explains the dip in the energy or magnetization density.

Since the magnitude of the dips in the probability densities scales exponentially with the size of the system, the dynamics in a canonical ensemble is tremendously slowed down. In the time series of Fig. 2 this is reflected by the increasing time the systems spends in the pure phases when the system size becomes larger. More formally the average time between flips (or, equivalently, the frequency of flips) sets an intrinsic time scale of the system, the autocorrelation time, which for canonical simulations grows exponentially with the system size – a severe problem in numerical simulations that will only be touched on in this lecture.

Rather, we will start out in the next section with a brief account of hysteresis effects and the method of thermodynamic integration and then focus mainly on thermodynamic equilibrium properties of the transition. The main body of this lecture is collected in Sect. 3, where the finite-size scaling behaviour at first-order transitions and its exploitation in analyses of computer simulations will be described. Section 4 is devoted to numerical computations of interface tensions, and in Sect. 5 we close with a brief summary.

2. Hysteresis effects and thermodynamic integration

In numerical simulations one necessarily considers finite systems. As a consequence no sharp jumps or singularities can develop. If the simulation time is large enough (i.e., much larger than the intrinsic time scale set by the autocorrelation time), equilibrium properties can be studied. At first-order phase transitions, however, the intrinsic autocorrelation times can be huge already for relatively small systems and, when heating or cooling the system too fast, hysteresis effects may be observed. This phenomenon is illustrated in Fig. 4(a) for the two-dimensional 10-state Potts model on a 50×50 square lattice. Shown are heating and cooling runs between $\beta = 1/k_B T = 1$ and 2 in 100 steps of $\Delta\beta = 0.01$, employing a single-hit Metropolis algorithm. For each β, 50 sweeps through the lattice were performed for a (very) short equilibration and another 500 sweeps for measuring and averaging the energy and other quantities (each run takes about 1 minute on a 733 MHz Pentium III). When heating up the system ($\beta = 2 \to 1$), it follows the low-temperature branch and slightly overheats, while when cooling down ($\beta = 1 \to 2$) it follow the high-temperature branch and we observe a somewhat more pronounced undercooling. When plotted together, this results in a clear hysteresis loop. By increasing the number of sweeps per β, the hysteresis loop would shrink in size and eventually one would approach the equilibrium curve. The vertical dotted line shows the exactly known location of the infinite-volume transition point $\beta_0 = \ln(1+\sqrt{10}) = 1.426\,062\,439\ldots$ and the values of the energies in the ordered ($E_o/V = -1.664\,253\ldots$) and disordered ($E_d/V = -0.968\,203\ldots$) phase, implying a latent heat of $\Delta E/V = 0.696\,050\ldots$. For comparison, we have also plotted low- and (dual) high-temperature series expansions up to order 31 which can be generated from the information given in Ref. [8] (for this plot, the series were simply summed up; for a more refined series analysis using partial differential approximants, see Ref. [8]).

While such a plot clearly indicates a phase transition around $\beta = 1.4 - 1.5$, its precise location would be difficult to read off from Fig. 4(a). A nice improvement is achieved by employing so-called thermodynamic integration to obtain the associated free energies of the low- and high-temperature branches (at least with conventional Monte Carlo simulation techniques, free energies cannot be obtained directly). Since the stable phase has the lower free energy, one can estimate the location of the phase transition by the crossing point of the two free-energy branches. More precisely, by recalling the relation $E = d\beta F/d\beta$, one computes for example for the high-temperature branch

$$\int_{\beta_1}^{\beta} d\beta' E(\beta') = \beta F(\beta) - \beta_1 F(\beta_1), \tag{1}$$

where the integral is approximated by summing up the measured energies. The integration constant fixing the overall normalization of the free energy is an additional input and has to be determined by some other means. In many cases this can be obtained by low-order series expansions, as was done here. By computing the low-temperature branch of the free energy in an analogous way, we arrive at the plot shown in Fig. 4(b), where the metastable part of the free-energy branches is indicated by the dashed lines. We

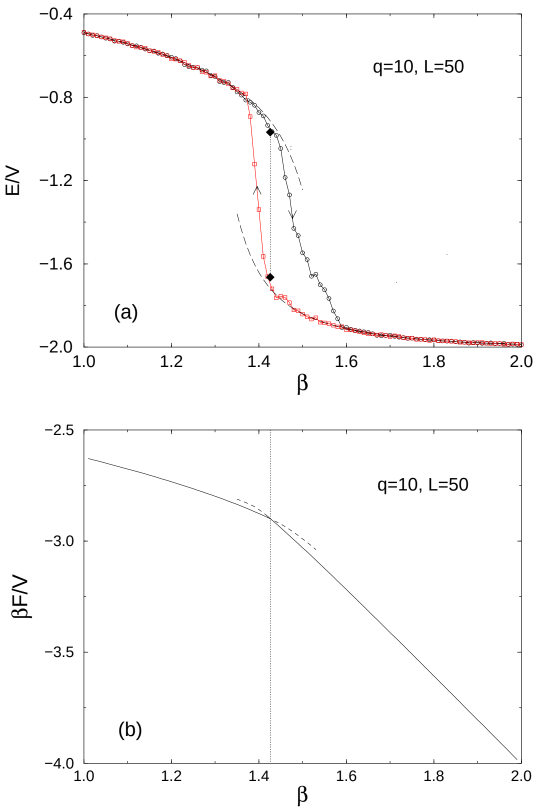

Figure 4. (a) Hysteresis loop in Monte Carlo simulations of the 2D 10-state Potts model on a 50×50 lattice. The heating and cooling protocols are described in the text. The dotted vertical line indicates the infinite-volume transition point and latent heat. The dashed curves show low- and (dual) high-temperature series expansions up to order 31. (b) The associated free energy obtained from the Monte Carlo data in (a) by thermodynamic integration.

see that the crossing point of the two free-energy branches agrees very well with the infinite-volume transition point β_0, with an accuracy of about 1%. The cusp at β_0 in Fig. 4(b) corresponds to the latent heat in Fig. 4(a).

3. Finite-size scaling

As pointed out already in the last section, in finite systems the number of degrees of freedom is finite and no sharp singularities can develop. Consequently, for instance the jump of the energy in a temperature-driven first-order phase transition is replaced in an equilibrated system by a smooth crossover, and the δ-function like divergence of the specific heat by a slightly displaced peak of finite width. As we shall argue below, the height of the peak scales with the volume V of the system and the width and displacement both decrease proportional to $1/V$, such that the integral over the peak is of order unity for all system sizes, as for a δ-function. Investigations of the finite-size scaling behaviour of first-order phase transitions started in the early eighties with work by Imry [9], Binder [10], and Fisher and Berker [11]. Subsequently many details were worked out [12, 13, 14, 15, 16, 17], and in the early nineties rigorous results for periodic boundary conditions could be derived [18, 19, 20], which is the simplest and best studied case of classical lattice systems. More recently also surface effects have been analyzed analytically [21, 22] and numerically [23].

3.1. SOME MODEL SYSTEMS

While most of the following arguments are quite general, to be specific we shall concentrate on one prototype model, namely the q-state Potts model with partition function

$$Z = \sum_{\{s_i\}} \exp(-\beta \mathcal{H}), \qquad \mathcal{H} = -J \sum_{\langle ij \rangle} \delta_{s_i s_j}, \qquad s_i = 1, \ldots, q, \tag{2}$$

where β is the inverse temperature in natural units, $J > 0$ is a ferromagnetic coupling constant and the sum runs over all nearest-neighbour pairs $\langle ij \rangle$ of a D-dimensional lattice which we shall take to be either square or cubic subject to periodic boundary conditions.

In two dimensions (2D) many exact results are known for this model in the infinite-volume limit [24]. First of all it is self-dual, meaning that equivalent properties are found at low and high inverse temperatures β and β^*, provided they are related by $[\exp(\beta) - 1][\exp(\beta^*) - 1] = q$. As function of temperature, self-duality predicts (by assuming a unique transition and equating β and β^*) a phase transition at $\beta_0 \equiv J/k_B T_0 = \ln(1 + \sqrt{q})$ from an ordered low-temperature to a disordered high-temperature phase, which is known to be of second order for $q \leq 4$ and of first order for $q \geq 5$. Right at the first-order transition point the average energy follows from self-duality as $(\hat{e}_o + \hat{e}_d)/2 = -(1 + 1/\sqrt{q})$, where $\hat{e}_o \equiv e_o(\beta_0)$ etc., and also the latent heat is known exactly [25], $\Delta\hat{e} \equiv \hat{e}_d - \hat{e}_o = 2(1 + 1/\sqrt{q}) \tanh(\Theta/2) \prod_{n=1}^{\infty} \tanh^2(n\Theta)$, where $2\cosh(\Theta) = \sqrt{q}$. Hence the energies at the transition are exactly known both in the coexisting disordered and ordered phases. For the specific heat, self-duality implies an exact expression for $\Delta C = \hat{C}_d - \hat{C}_o = \beta_0^2 \Delta\hat{e}/\sqrt{q}$, but the average and thus the values of $\hat{C}_d$ and $\hat{C}_o$ are not known analytically. Also exactly known is the correlation length in the disordered phase at the transition point [26, 27, 28], $\xi_d(\beta_0)$, and the (reduced) order-disorder interfacial tension which can be related to this correlation length [29], $\hat{\sigma}_{od} \equiv \beta_0 \sigma_{od} = 1/2\xi_d(\beta_0)$.

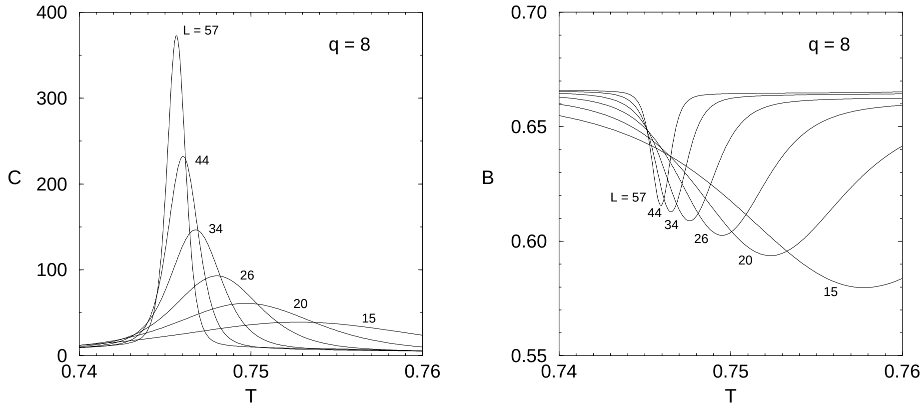

Figure 5. FSS behaviour of the traditional observables, specific heat C and Binder parameter B, for the 2D 8-state Potts model. The infinite-volume transition temperature is $T_0 = 1/\ln(1+\sqrt{8}) = 0.744\,904\,455\ldots$.

In three dimensions (3D) no exact results are available, but numerical evidence strongly suggests that the transition is of first order for $q \geq 3$ (with the precise crossover point to a second-order transition located somewhere between $q = 2$ and 3) [30].

3.2. FINITE-SIZE SCALING OF STANDARD OBSERVABLES

The traditional way of locating first-order transition points is based on the scaling behaviour of the maximum of the specific heat $C(\beta, V) = \beta^2 V(\langle e^2\rangle - \langle e\rangle^2)$ and the minimum of the Binder parameter $B(\beta, V) = 1 - \langle e^4\rangle/3\langle e^2\rangle^2$. For an illustration see Fig. 5 where data for the 2D 8-state Potts model are shown. In both plots we see that the peaks of C and the wells of B are shifted and become narrower with increasing system size $V = L^2$. If the volume is cubic or nearly cubic the location of the extrema is typically displaced by an amount $O(V^{-1})$ with respect to the actual infinite-volume transition point and one may try to estimate β_0 from the finite-volume results by extrapolations in $1/V$. And for the specific heat we can already guess from Fig. 5 that the peak height indeed increases proportional to the volume.

What is the reason for this behaviour? In the following we shall give three arguments of increasing complexity and, at the same time, increasing rigor. In fact, at least for Potts models with sufficiently large q, the final argument based on Pirogov-Sinai theory is a rigorous statement.

3.2.1. *Histogram argument*

This is the most straightforward way to see that the maximum of the specific-heat peak should scale proportional to the volume of the system.

Accepting that, due to phase coexistence, the energy density exhibits a double-peak structure with the two peaks approximately separated by a distance $V\Delta\hat{e}$, where $\Delta\hat{e}$ is the non-vanishing (infinite volume) latent heat of the transition, one simply estimates the leading contribution to the variance $\sigma_E^2 = \langle (E - \langle E \rangle)^2 \rangle \approx (V\Delta\hat{e}/2)^2$ from the (squared) half-width of the double peak, that is the separation of the two peaks. For the specific heat $C = \beta^2 V(\langle e^2 \rangle - \langle e \rangle^2) = \beta^2 V \langle (e - \langle e \rangle)^2 \rangle = \beta^2 \langle (E - \langle E \rangle)^2 \rangle / V$ this implies $C \approx (\beta\Delta\hat{e}/2)^2 V$ which, with $\beta \approx \beta_0$, is indeed the correct asymptotic FSS behaviour, including the prefactor, as will be shown below more rigorously. This explains in the most direct and simplest way how phase coexistence and a non-vanishing latent heat are related to the scaling behaviour $C \propto V$ of the specific heat.

3.2.2. *Tunneling argument*

The leading terms can be derived in somewhat more detail by considering a simple two-state model where one assumes that the system spends a fraction W_o of the total time in the ordered phases with energy e_o and a fraction $W_d = 1 - W_o$ in the disordered phase with energy e_d. Within this simple picture the flips from one state to the other are approximated by sharp jumps and all fluctuations within the phases are neglected. Energy moments can then be expressed as $\langle e^n \rangle = W_o e_o^n + (1 - W_o) e_d^n$, and for the specific heat we find

$$C = V\beta^2(\langle e^2 \rangle - \langle e \rangle^2) = V\beta^2 W_o (1 - W_o) \Delta e^2. \tag{3}$$

It is now easy to derive that C has a maximum

$$C_{\max} = V\beta_0^2\,(\Delta\hat{e}/2)^2 \tag{4}$$

for $W_o = W_d = 1/2$, i.e., for an energy distribution with two peaks of equal weight. Here we have defined $\Delta\hat{e} \equiv \hat{e}_d - \hat{e}_o$. The peak location

$$\beta_{C_{\max}} = \beta_0 - \ln q / V\Delta\hat{e} + \ldots \tag{5}$$

follows from the expansion $\ln(W_o/W_d) = \ln q + V\beta(f_d - f_o) = \ln q + V\Delta\hat{e}(\beta - \beta_0) + \ldots$ and equating this to $\ln(W_o/W_d) = \ln 1 = 0$. Similarly, the minimum of the Binder parameter,

$$B_{\min} = 1 - (\hat{e}_o/\hat{e}_d + \hat{e}_d/\hat{e}_o)^2/12, \tag{6}$$

is found at a weight ratio $W_o/W_d = \hat{e}_d^2/\hat{e}_o^2 < 1$, implying

$$\beta_{B_{\min}} = \beta_0 - \ln(q\hat{e}_o^2/\hat{e}_d^2)/V\Delta\hat{e} + \ldots. \tag{7}$$

This simple argument thus not only explains the qualitative asymptotic behaviour as a function of the system size V, but also predicts the prefactors expressed in term of $\hat{e}_o$, $\hat{e}_d$, β_0, and q.

3.2.3. *Pirogov-Sinai argument*
Let us finally recapitulate a rigorous derivation [18, 19] which is based on the observation that the partition function of a model such as (2), describing the coexistence of one disordered and q ordered phases, can be written for large enough q as

$$Z_{\rm per}(\beta,V) = \left(\sum_{m=0}^{q} e^{-\beta V f_m(\beta)}\right)\left[1+\mathcal{O}\left(V e^{-L/L_0}\right)\right], \tag{8}$$

where the subscript "per" indicates that here and in the following we shall always assume periodic boundary conditions. This should be emphasized because the choice of boundary conditions is very crucial in the present context. The free energy densities $f_m(\beta)$, $m = 0,\ldots,q$, are defined as meta-stable quantities in such a way that they are equal to the idealized infinite-volume free energy density $f(\beta)$ if m is stable and strictly larger than $f(\beta)$ if m is unstable [18, 19]. The constant $L_0 < \infty$ governing the exponentially small correction term in (8) is of the order of the (largest, but finite) correlation length at β_0.

Taking into account that the q ordered phases are equivalent by symmetry and neglecting for the moment the exponentially small corrections this can be rewritten as

$$\begin{aligned} Z_{\rm per}(\beta,V) &\simeq e^{-\beta V f_d} + q e^{-\beta V f_o} \\ &= 2\sqrt{q} e^{-\beta V (f_d+f_o)/2} \cosh\left(\beta V \frac{f_d-f_o}{2} + \frac{1}{2}\ln q\right), \end{aligned} \tag{9}$$

where $f_d(\beta) \equiv f_0(\beta)$ and $f_o(\beta) \equiv f_m(\beta)$, $m = 1,\ldots,q$, denote the infinite-volume free energy densities of the pure disordered and ordered phases, respectively. Notice that exponentially small finite-size corrections of the pure phase quantities are already contained in the error term of eq. (8). From (9) it is easy to derive formulas for the energy $e(\beta,V) = -d\ln Z_{\rm per}(\beta,V)/d\beta$,

$$e(\beta,V) = \frac{e_d+e_o}{2} - \frac{e_d-e_o}{2}\tanh\left(\beta V\frac{f_d-f_o}{2} + \frac{1}{2}\ln q\right), \tag{10}$$

and specific heat $C(\beta,V) = -\beta^2 de(\beta,V)/d\beta$,

$$\begin{aligned} C(\beta,V) &= \frac{C_d+C_o}{2} - \frac{C_d-C_o}{2}\tanh\left(\beta V\frac{f_d-f_o}{2} + \frac{1}{2}\ln q\right) \\ &+ \beta^2 V\left(\frac{e_d-e_o}{2}\right)^2 \cosh^{-2}\left(\beta V\frac{f_d-f_o}{2} + \frac{1}{2}\ln q\right), \end{aligned} \tag{11}$$

where all quantities are evaluated at inverse temperature β. For fixed $\beta < \beta_0$ ($\beta > \beta_0$) we have $f_d < f_o$ ($f_o < f_d$), such that in the infinite-volume limit $V \to \infty$ the hyperbolic tangent approaches -1 ($+1$) and the hyperbolic cosine tends to infinity. The asymptotic limits of eqs. (10) and (11) are hence $e(\beta, V) \to e_d(\beta)$ ($e_o(\beta)$) and $C(\beta, V) \to C_d(\beta)$ ($C_o(\beta)$), respectively, as expected on physical grounds. The range of the smooth interpolation between the ordered and disordered phase is governed by the scaling variable

$$x = \beta V \frac{f_d - f_o}{2} + \frac{1}{2} \ln q = V \frac{\hat{e}_d - \hat{e}_o}{2} (\beta - \beta_0) + \frac{1}{2} \ln q + \ldots, \tag{12}$$

showing that the rounding of the transition takes place over a range $\Delta\beta = |\beta - \beta_0| \propto 1/V$.

Right at the infinite-volume transition point β_0, we have phase coexistence and the two free energies are equal, $f_d(\beta_0) = f_o(\beta_0)$. Inserting $\tanh(\frac{1}{2} \ln q) = (q-1)/(q+1)$ and $\cosh^{-2}(\frac{1}{2} \ln q) = 1 - \tanh^2(\frac{1}{2} \ln q) = 4q/(q+1)^2$, we obtain

$$e(\beta_0, V) = \frac{q\hat{e}_o + \hat{e}_d}{q+1}, \tag{13}$$

and

$$C(\beta_0, V) = \frac{q\hat{C}_o + \hat{C}_d}{q+1} + \frac{4q}{(q+1)^2} V \left(\frac{\Delta\hat{s}}{2}\right)^2, \tag{14}$$

where we have introduced the transition entropy

$$\Delta\hat{s} = \beta_0 \Delta\hat{e}, \qquad \Delta\hat{e} = \hat{e}_d - \hat{e}_o > 0, \tag{15}$$

and denoted quantities evaluated at β_0 by a "hat", e.g. $\hat{e}_d = e_d(\beta_0)$. Notice that apart from the neglected exponential corrections indicated in (8) the formulas for $e(\beta_0, V)$ and $C(\beta_0, V)$ are exact. In particular we see that $e(\beta_0, V)$ has *only* exponentially small finite-size corrections. This implies that the energy curves for different lattice sizes should cross to a very good approximation in the point $(\beta_0, (q\hat{e}_o + \hat{e}_d)/(q+1))$. Turning the argument around this implies that using the crossing points of the energy for different lattice sizes as a definition for a pseudo transition point, these points should deviate from β_0 by only an exponentially small amount. We shall come back to this definition with a slightly different argumentation.

At the point $\beta_{\rm eqw}$ where the two phases contribute with equal weight, we have $e^{-\beta V f_d(\beta)} = q e^{-\beta V f_o(\beta)}$ such that $x = \beta V \frac{f_d - f_o}{2} + \frac{1}{2} \ln q = 0$, and eqs. (10) and (11) immediately simplify to $e_{\rm eqw} = e(\beta_{\rm eqw}, V) = (e_d + e_o)/2$ and $C_{\rm eqw} = C(\beta_{\rm eqw}, V) = (C_d + C_o)/2 + \beta_{\rm eqw}^2 V (\Delta e/2)^2$, where e_d, e_o, etc. are evaluated at $\beta_{\rm eqw}$. By inserting Taylor expansions around β_0, e.g. $\beta f_d(\beta) = \beta_0 \hat{f}_d + \hat{e}_d(\beta - \beta_0) - \hat{C}_d(\beta - \beta_0)^2/2\beta_0^2 + \ldots$, and solving for $x = 0$

one obtains [31]

$$\beta_{\rm eqw} = \beta_0 - \frac{\beta_0}{V\Delta\hat{s}}\ln q + \frac{\beta_0}{(V\Delta\hat{s})^2}\frac{\Delta\hat{C}}{2\Delta\hat{s}}(\ln q)^2 + \mathcal{O}(1/V^3), \tag{16}$$

and

$$C_{\rm eqw} = V\left(\frac{\Delta\hat{s}}{2}\right)^2 + \frac{(\Delta\hat{C}-\Delta\hat{s})\ln q}{2} + \frac{\hat{C}_d+\hat{C}_o}{2} + \mathcal{O}(1/V), \tag{17}$$

with $\Delta\hat{C} = \hat{C}_d - \hat{C}_o$. Similarly straightforward but rather tedious calculations yield the asymptotic $1/V$ expansions of the specific-heat maximum, Binder parameter minimum etc. For the location of the specific-heat maximum one finds [31, 32]

$$\begin{aligned}\beta_{C_{\rm max}} &= \beta_0 - \frac{\beta_0}{V\Delta\hat{s}}\ln q + \frac{\beta_0}{(V\Delta\hat{s})^2}\left[\frac{\Delta\hat{C}}{2\Delta\hat{s}}\Big((\ln q)^2 - 12\Big) + 4\right] \\ &+ a_3/V^3 + a_4/V^4 + \mathcal{O}(1/V^5),\end{aligned} \tag{18}$$

and

$$\begin{aligned}C_{\rm max} &= V\left(\frac{\Delta\hat{s}}{2}\right)^2 + \frac{(\Delta\hat{C}-\Delta\hat{s})\ln q}{2} + \frac{\hat{C}_d+\hat{C}_o}{2} + \mathcal{O}(1/V) \\ &= C_{\rm eqw} + \mathcal{O}(1/V).\end{aligned} \tag{19}$$

Notice that $\beta_{C_{\rm max}} = \beta_{\rm eqw} + \mathcal{O}(1/V^2) \stackrel{\rm 2D\ Potts}{>} \beta_{\rm eqw}$ and $C_{\rm max} = C_{\rm eqw} + \mathcal{O}(1/V)(> C_{\rm eqw}$ by definition). In the asymptotic expansion (18) also the higher-order correction terms $\propto 1/V^3$ and $\propto 1/V^4$ are indicated which both have also been calculated explicitly [33]. As they turn out to be rather complicated, however, here we only give

$$\begin{aligned}a_3 = \frac{\beta_0}{\Delta\hat{s}^3}\Bigg[&8\frac{\hat{C}_d+\hat{C}_o}{\Delta\hat{s}} - 4\frac{\kappa_d^{(3)}+\kappa_o^{(3)}}{\Delta\hat{s}} + \left(4 - 8\frac{\Delta\hat{C}}{\Delta\hat{s}}\right)\ln q \\ &\left(\frac{1}{6}\frac{\kappa_d^{(3)}-\kappa_o^{(3)}}{\Delta\hat{s}} - \frac{1}{2}\frac{\Delta\hat{C}^2}{\Delta\hat{s}^2}\right)\Big((\ln q)^3 - 36\ln q\Big)\Bigg].\end{aligned} \tag{20}$$

As a new feature also the higher cumulants $\kappa_d^{(3)}$ and $\kappa_o^{(3)}$ enter as parameters (as well as $\kappa_d^{(4)}$ and $\kappa_o^{(4)}$ in a_4, and so on) which are defined through the Taylor expansion of the free energy around β_0, e.g.,

$$-\beta f_d(\beta) = -\beta_0 f_d(\beta_0) + \sum_{n=1}(-1)^n\kappa_d^{(n)}(\beta/\beta_0 - 1)^n/n!. \tag{21}$$

For low orders, special cases are $\kappa_d^{(1)} = \beta_0 e_d(\beta_0)$, $\kappa_d^{(2)} = c_d(\beta_0)$, and $\kappa_d^{(3)} = \beta_0^3 \langle (E - \langle E \rangle_d)^3 \rangle_d / V$. Recall, that from $n = 4$ on the relation between cumulants $\kappa_n \equiv V \kappa_d^{(n)}$ and central moments $\mu_n = V \mu_d^{(n)} = \langle (E - \langle E \rangle_d)^n \rangle$ is more complicated, e.g., $\kappa_4 = \mu_4 - 3\mu_2^2$, $\kappa_5 = \mu_5 - 10\mu_2\mu_3$, $\kappa_6 = \mu_6 - 15\mu_2\mu_4 - 10\mu_3^2 + 30\mu_2^3, \ldots$.

Similar asymptotic expansions can be derived for quantities related to the Binder parameter minimum [31, 32], confirming the leading-order results (6) and (7) obtained with the tunneling argument. For a comparison with simulation data see Fig. 6.

3.2.4. *Double-Gaussian approximation*

Early work on FSS of first-order phase transitions focused directly on the double-peak of the energy density and employed a double-Gaussian approximation to it [13, 14, 15]. In light of the preceding exact treatment the properly normalized ansatz[1] parametrized by the infinite-volume energy $e_{d,o}(\beta)$ and specific heat $c_{d,o}(\beta)$in the pure phases would read,

$$\begin{aligned} P_{\beta,V}(e) &= e^{-\beta V f_d} \sqrt{\frac{\beta^2 V}{2\pi C_d}} e^{-\frac{\beta^2 V (e-e_d)^2}{2C_d}} + q e^{-\beta V f_o} \sqrt{\frac{\beta^2 V}{2\pi C_o}} e^{-\frac{\beta^2 V (e-e_o)^2}{2C_o}} && (22) \\ &= A \left[\frac{A_d}{\sqrt{C_d}} e^{-\frac{\beta^2 V (e-e_d)^2}{2C_d}} + q \frac{A_o}{\sqrt{C_o}} e^{-\frac{\beta^2 V (e-e_o)^2}{2C_o}} \right] && (23) \\ &= e^{-\beta V f_d} \sqrt{\frac{\beta^2 V}{2\pi}} \left[\frac{1}{\sqrt{C_d}} e^{-\frac{\beta^2 V (e-e_d)^2}{2C_d}} + \frac{\tilde{q}}{\sqrt{C_o}} e^{-\frac{\beta^2 V (e-e_o))^2}{2C_o}} \right], && (24) \end{aligned}$$

where $A = e^{-\beta V (f_d + f_o)/2} \sqrt{\beta^2 V / 2\pi}$, $A_d = e^{-\beta V \Delta f}$ and $A_o = e^{+\beta V \Delta f}$ with $\Delta f = f_d - f_o$, and $\tilde{q} = q e^{\beta V (f_d - f_o)} = e^{2x}$, where $x = \frac{1}{2} \ln q + \frac{1}{2} \beta V (f_d - f_o)$ is the scaling variable introduced earlier in (12). Since each Gaussian peak in the representation (22) is normalized to unit area, by integrating $P_{\beta,V}(e)$ one recovers $Z_{\rm per}(\beta, V)$ of (8). Within the double-Gaussian approximation one then proceeds by calculating the energy moments as

$$\langle e^n \rangle = \int_{-\infty}^{\infty} de\, e^n P_{\beta,V}(e) / \int_{-\infty}^{\infty} P_{\beta,V}(e). \qquad (25)$$

This gives $\langle e \rangle = (e_d + \tilde{q} e_o)/(1 + \tilde{q})$, $\langle e^2 \rangle = (e_d^2 + \tilde{q} e_o^2)/(1 + \tilde{q}) + (C_d + \tilde{q} C_o)/[V \beta^2 (1 + \tilde{q})]$, and $C = \beta^2 V (\langle e^2 \rangle - \langle e \rangle^2) = \beta^2 V (\tilde{q}/(1 + \tilde{q})^2)(e_d - e_o)^2 + (C_d + \tilde{q} C_o)/(1 + \tilde{q})$, which may be recast into the form

$$\langle e \rangle \;=\; (\tilde{q}^{-1/2} e_d + \tilde{q}^{1/2} e_o)(\tilde{q}^{-1/2} + \tilde{q}^{1/2})$$

[1] In the original papers the different assumption $P_{\beta,V}(e_o)/P_{\beta,V}(e_d) = q$ was made, leading to different predictions for higher powers in $1/V$ of the FSS behaviour.

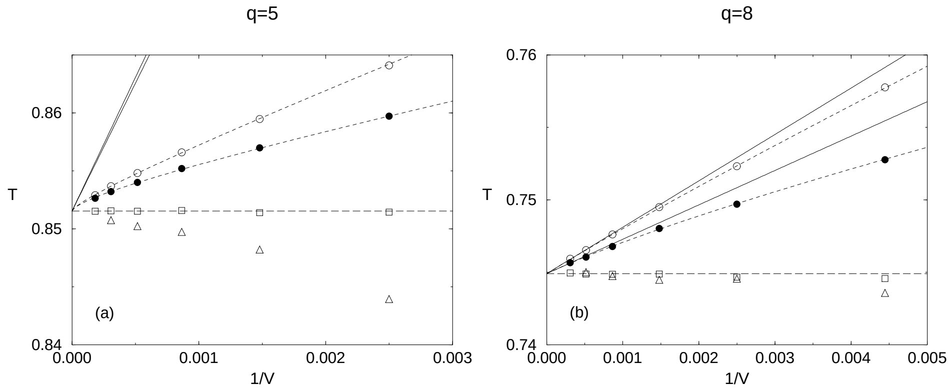

Figure 6. 2D q-state Potts model: FSS behaviour of the finite-volume transition points defined by the Binder-parameter minimum ($\circ$) and the specific-heat maximum ($\bullet$). The solid straight lines are the exactly known $1/V$ corrections corresponding to $\circ$ and $\bullet$, and the dashed, almost interpolating curves show exponential fits (including the $1/V$ corrections) to these data. Note that the $(1/V)^2$ corrections are almost invisible on this scale and in any case point in the "wrong" upward direction. The long dashed horizontal lines indicate the exact infinite-volume transition points. Also shown are for comparison results from the number-of-phases criterion ($\triangle$) and the ratio-of-weights parameter ($\square$), discussed below.

$$
\begin{aligned}
&= \left[-\frac{\tilde{q}^{1/2}-\tilde{q}^{-1/2}}{2}(e_d-e_o)+\frac{\tilde{q}^{1/2}+\tilde{q}^{-1/2}}{2}(e_d+e_o)\right]/(\tilde{q}^{-1/2}+\tilde{q}^{1/2}) \\
&= \frac{e_o+e_d}{2}-\frac{e_d-e_o}{2}\tanh(x), \qquad (26)
\end{aligned}
$$

which is identical to (10). Similarly, using that

$$
\frac{\tilde{q}}{(1+\tilde{q})^2}=\frac{1}{\tilde{q}^{1/2}+\tilde{q}^{-1/2}}=\frac{1}{4\cosh^2(x)}, \qquad (27)
$$

one recovers eq. (11) for the specific heat. Consequently, also the leading FSS predictions must be the precisely the same.

Since for a Gaussian distribution all higher cumulants $\kappa_{o,d}^{(n)}$ with $n \geq 3$ vanish, however, the double-Gaussian approximation can self-consistently only reproduce the leading terms of the asymptotic finite-size scaling expansions. This is the main difference between the last two approaches.

3.2.5. *Exponentially small correction terms*

Of course, since we are dealing with asymptotic expansions (which at a given order approach the exact result as $V \to \infty$, but not necessarily converge with increasing order for a fixed volume V), the question arises whether the higher orders given in (18) pay off at all. Moreover, when comparing with actual numerical data, we should keep in mind that we have

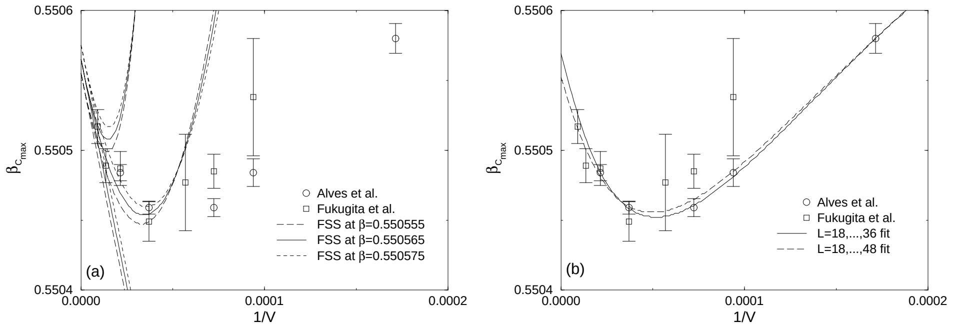

Figure 7. 3D 3-state Potts model: (a) FSS behaviour of the specific-heat maximum locations together with the predicted FSS power-law expansion in $1/V$ and (b) fits of the form $\beta_{c_{\max}} = \beta_0 + a_1/V + a\exp(-bL)$ [30].

so far completely neglected the exponential corrections indicated in the initial formula (8) for Z_{per}. While asymptotically negligible in comparison with powers of $1/V$, for moderate system sizes exponential corrections may indeed be comparable in size (what is "moderate" depends on both, the parameter L_0 in (8), being of the order of the largest correlation length, and an unknown prefactor). That this is indeed the case for 2D and 3D Potts models is demonstrated in Figs. 6 and 7, where we see that power-law corrections alone cannot account for the numerical data. Only when additional exponential corrections are taken into account, good fits to the data can be achieved.

3.3. IMPROVED OBSERVABLES WITHOUT POWER-LAW CORRECTIONS

As we have seen in the last subsection, apart from random statistical errors the data are in general also systematically affected by exponentially small corrections which are often difficult to take into account in practice. This renders the extrapolations of finite-volume data not always reliable, and it is therefore desirable to find definitions for the finite-volume transition points that do *not* involve any corrections in powers of $1/V$.

3.3.1. *Number-of-phases criterion*

One such definition is based on the observation that the partition function of a model such as (2), describing the coexistence of one disordered and q ordered phases, can be written for large enough q in the simple form (8). This representation implies (see also Refs. [34, 31]) that in the infinite-volume limit the parameter

$$N(\beta, V) \equiv Z_{\text{per}}(\beta, V) e^{\beta f(\beta) V} \tag{28}$$

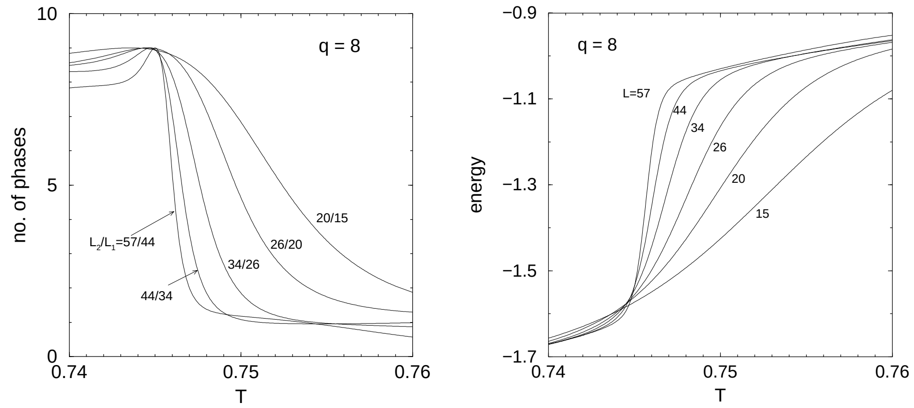

Figure 8. FSS behaviour of the number-of-phases parameter $N(\beta, V_1, V_2)$ defined in eq. (29) and the energy $e = E/V$ for the 2D 8-state Potts model.

is equal to the number of stable phases at the inverse temperature β, i.e., $N(\beta) \equiv \lim_{V\to\infty} N(\beta, V) = q$ in the ordered phase, $N(\beta) = 1$ in the disordered phase, and $N(\beta) = q + 1$ at the transition point β_0 where the phases coexist. A natural definition of a finite-volume transition point $\beta_0(V)$ would thus be the point where $N(\beta, V)$ is maximal. Due to the form of the correction term in (8) (and similar expressions for derivatives [18, 19]), this definition would lead to only *exponentially* small shifts of $\beta_0(V)$ with respect to the infinite-volume transition point β_0.

The free energy $f(\beta)$ in (28), however, is only defined in the thermodynamic limit and hence not accessible to numerical simulations. It is therefore necessary to eliminate this term by, e.g., studying two systems of different sizes V_1 and $V_2 = \alpha V_1$ and forming a suitable ratio. Instead of (28), this leads to the following definition [34, 31] of the *number-of-phases* parameter:

$$N(\beta, V_1, V_2) = \left[\frac{Z_{\rm per}(\beta, V_1)^\alpha}{Z_{\rm per}(\beta, V_2)} \right]^{\frac{1}{\alpha-1}} . \tag{29}$$

By inserting (8) it is straightforward to verify that with increasing temperature $N(\beta, V_1, V_2)$ smoothly interpolates between the values q, $q + 1$, and 1. The locations of the maxima define the desired finite-volume transition points $\beta_0(V_1, V_2)$ which for brevity will be denoted by $\beta_{V/V}$. For an approximately fixed ratio $\alpha = V_2/V_1$, these pseudo-transition points $\beta_{V/V}$ are displaced from β_0 by only an exponentially small amount. Actual simulation results for the 2D 8-state Potts model with $\alpha = V_2/V_1 \approx 1.6$ are shown in Fig. 8. By differentiating $\ln N(\beta, V_1, V_2)$ with respect to β one readily sees that determining $\beta_{V/V}$ amounts to solving $\alpha E(\beta_{V/V}, V_1) = E(\beta_{V/V}, V_2)$

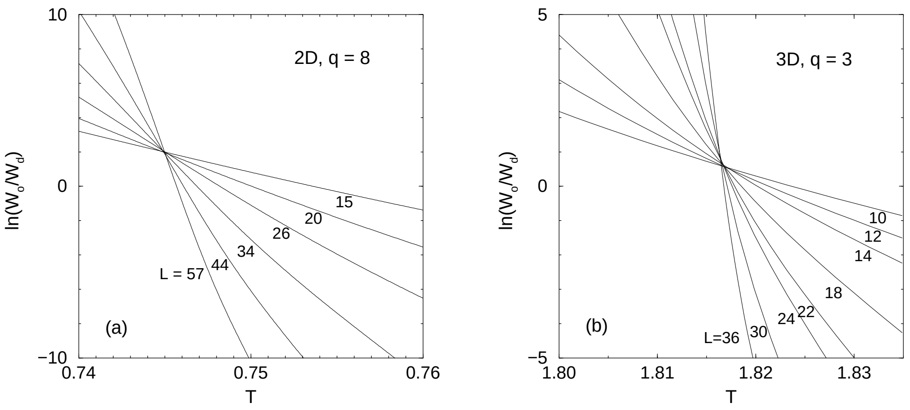

Figure 9. FSS behaviour of the ratio-of-weights parameter $R(\beta, V)$ defined in eq. (31) for the (a) 2D 8-state and (b) 3D 3-state Potts model.

or $e(\beta_{V/V}, V_1) = e(\beta_{V/V}, V_2)$, i.e., to locating the crossing point of the internal energies per site, $e \equiv E/V$, of the two lattices of different size, as anticipated earlier. The latter criterion is often more convenient to apply in practice.

3.3.2. *Ratio-of-weights parameter*

In both versions, however, the numerical determination of $\beta_{V/V}$ requires simulations of two different lattices. In order to reduce the numerical effort we have therefore proposed in Ref. [34] another definition of a finite-volume transition point which requires data from one lattice only. Its definition exploits the fact that at the infinite-volume transition point all phases coexist and therefore all free energies $f_m(\beta)$ are equal, so that in the limit of large volumes eq. (8) with $f_0 \equiv f_d$ implies

$$w_o(\beta_t, V) \equiv \sum_{m=1}^{q} e^{-\beta_t f_m(\beta_t) V} = q e^{-\beta_t f_d(\beta_t) V} \equiv q w_d(\beta_t, V), \tag{30}$$

where w_o and w_d are the associated statistical weights of the coexisting phases. A natural definition of a finite-volume transition point β_W is thus the point where the ratio of the total weight of the q ordered phases to the weight of the disordered phase approaches q. More precisely we introduce the *ratio-of-weights* parameter

$$R(\beta, V) \equiv W_o/W_d \equiv \sum_{E<E_{\rm cut}} P_{\beta,V}(E) \Big/ \sum_{E \geq E_{\rm cut}} P_{\beta,V}(E), \tag{31}$$

where $P_{\beta,V}(E)$ are the (double-peaked) energy histograms, and determine β_W by solving

$$R(\beta_W, V) = q. \tag{32}$$

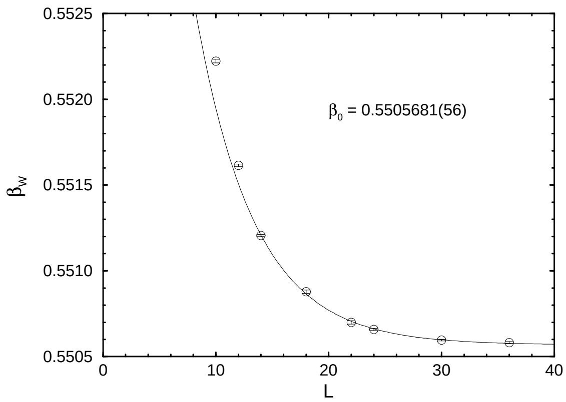

Figure 10. FSS behaviour of the pseudo-transition points β_W defined in eqs. (31) and (32) for the 3D 3-state Potts model together with an exponential fit of the form $\beta_W = \beta_0 + a\exp(-bL)$.

The parameter $E_{\rm cut}$ in (31) is defined by reweighting [35, 36] the energy histogram to the temperature where the two peaks of $P_{\beta,V}(E)$ have equal height and then taking $E_{\rm cut}$ as the energy at the minimum between the two peaks; for an example see Fig. 3. Other definitions of $E_{\rm cut}$ would be reasonable as well, as for example the internal energy at the temperature where the specific heat is maximal. Since it is expected that the relative height of the minimum between the two peaks decreases like $\exp(-2\beta\sigma L^{d-1})$ as $L \to \infty$, all these definitions do in fact only differ by exponentially small corrections and it is a matter of practical convenience to choose $E_{\rm cut}$. In Fig. 9(a) the logarithm of the ratio-of-weights parameter $R(V,\beta)$ for the 2D 8-state Potts model is plotted as a function of temperature. As is demonstrated in Fig. 6(b), the expected exponential corrections of the finite-volume transition points β_W are hardly resolvable in this case. Also at the very weak first-order transition for $q = 5$, with an extremely large, but finite pure-phase correlation length $\xi_d \approx 2500$, β_W almost hits the exactly known value of β_0 already for very small system sizes $L \ll \xi_d$, cf. Fig. 6(a). This enormous accuracy, however, is probably accidental and presumably caused by an almost vanishing amplitude. As another example, Figs. 9(b) and 10 show results for the 3D 3-state Potts model which also exhibits a weak first-order transition (with $\xi_d \approx 10 - 11$). Here the exponential corrections are clearly detectable.

In (32) we have assumed that the number of ordered phases, q, is known by general arguments. If this is not the case, one may use the crossing points $\beta_{W/W}$ satisfying $R\left(\beta_{W/W}, V_1\right) = R\left(\beta_{W/W}, V_2\right)$ as estimates for β_0.

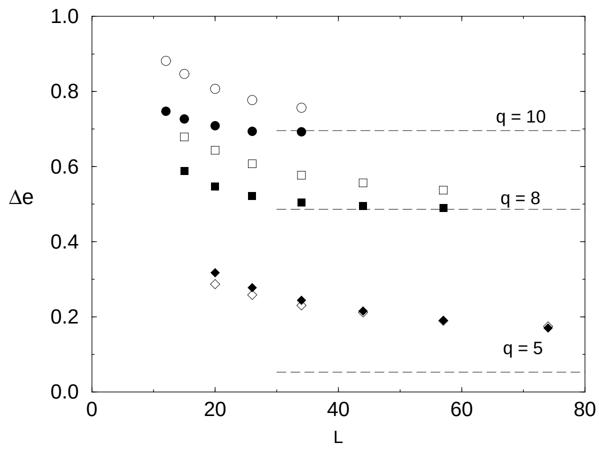

Figure 11. The finite-volume latent heat Δe of the 2D q-state Potts model vs linear lattice size L. The open symbols show the traditional estimates from the peak locations of $P_{V,\beta}(E)$, and the filled symbols follow from the slopes of the ratio-of-weight parameter. The dashed horizontal lines show the exactly known infinite-volume limits [24, 25].

The value of R at the crossing point then gives the ratio of the number of coexisting ordered and disordered phases. This, however, requires again the simulation on two lattices of different size.

3.3.3. *Improved estimator for the latent heat*

The ratio-of-weights method leads naturally to a finite-volume definition of the latent heat [31] which also should have only exponentially small corrections with respect to the infinite volume limit. Since

$$\ln(w_o/w_d) = -\beta V(f_o - f_d), \tag{33}$$

the slopes of $R(V,\beta)$ in Fig. 4 at the crossing point may be used to define

$$\Delta e(V) = e_d(V) - e_o(V) = \frac{d}{d\beta}\ln(W_o/W_d)/V = -\frac{1}{T^2}\frac{d}{dT}\ln(W_o/W_d)/V. \tag{34}$$

The resulting estimates $\Delta e(V)$ for the 2D q-state Potts model are plotted in Fig. 11 and compared with the traditional definition based on the peak locations of $P_{\beta,V}(E)$ [32]. For strong first-order transitions ($q = 8$ and 10) the asymptotic limit is indeed reached much faster with the new definition. For a very weak transition ($q = 5$), on the other hand, both methods yield comparable estimates which are still far away from the limiting value, indicating the importance of exponential corrections for this quantity. As

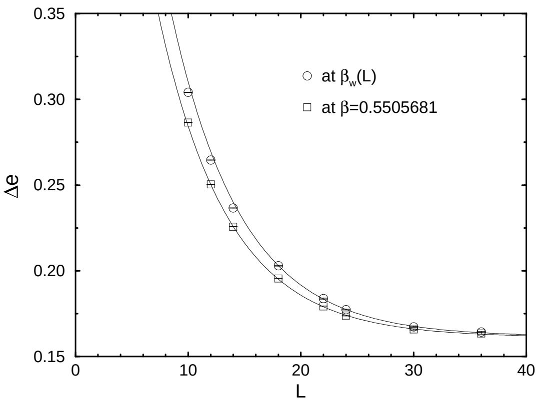

Figure 12. FSS behaviour of the latent heat for the 3D 3-state Potts model derived from the ratio-of-weights method. The continuous lines are fits of the form $\Delta e(L) = \Delta e(\infty) + a\exp(-bL)$.

can be seen in Fig. 12, also for the 3D Potts model the expected exponential corrections are clearly visible.

4. Interfacial tension

A quantity of central importance for the kinetics of first-order phase transitions is the interface tension σ between the coexisting phases [3, 4]. As discussed earlier, on finite periodic lattices of size L^d, this is reflected by a double-peak structure of the probability distribution for the energy or magnetization, with the minimum $\propto \exp(-2\beta\sigma L^{d-1})$ between the two peaks dominated by mixed phase configurations with two interfaces contributing an excess free energy of $2\sigma L^{d-1}$. This suggests [10, 37] to extract the reduced interface tension $\hat{\sigma} = \beta\sigma$ from the infinite volume limit of

$$2\hat{\sigma}^{(L)} = \frac{1}{L^{d-1}} \ln(P_{\rm max}^{(L)}/P_{\rm min}^{(L)}). \tag{35}$$

For accurate results the system has to travel many times between the two peaks, which is a serious problem in canonical simulations of strong first-order transitions (large σ). But for example multicanonical sampling [38, 39, 36] is just designed for this purpose since it gives the same relative errors for $P_{\rm max}^{(L)}$ and $P_{\rm min}^{(L)}$ and thus optimizes the error on $\hat{\sigma}^{(L)}$. As an example, in Fig. 13 data for $\hat{\sigma}^{(L)}$ are shown for the 2D 10-state Potts model. The lower bended curve shows the results obtained from following the traditional way of first reweighting the histogram to equal-peak height, cf. Fig. 3, and then computing the ratio in (35). Alternatively, one may either compute the ratio

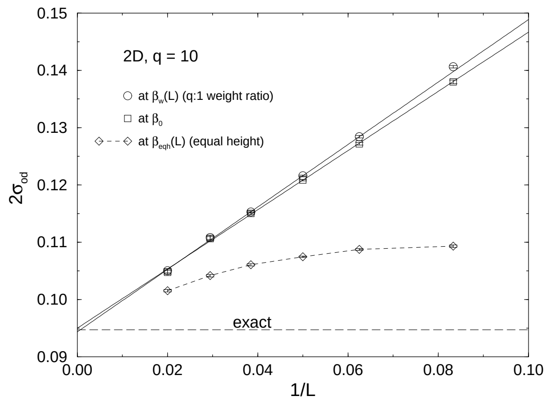

Figure 13. FSS behaviour of the interface tension for the 2D 10-state Potts model.

at the transition point β_0 (if it is known with high enough precision or, as in the 2D Potts model, even exactly) or at the pseudo-transition points $\beta_W(L)$ which deviate from β_0 only by an exponentially small amount. As can be inspected in Fig. 13, empirically the FSS behaviour is much cleaner in the latter two cases, enabling more precise extrapolations to the infinite-volume limit. For the data shown in Fig. 13, we obtained $2\hat{\sigma}_{od} = 0.09498(31)$ at β_0 and $2\hat{\sigma}_{od} = 0.09434(40)$ at $\beta_W(L)$ [40], in good agreement with the exact result $2\hat{\sigma}_{od} = 0.094\,701\ldots$ to be discussed next.

Using this so-called histogram method, interface tensions have been estimated for a variety of models (2D and 3D q-state Potts models [41, 42, 43, 44, 45, 46, 47, 31], disordered ferromagnets [48], $N_t = 2$ SU(3) lattice gauge theory [42, 49], Ising model below T_c in 2D and 3D [50], 2D ϕ^4 model [51]). A few of the numerical results for the 2D q-state Potts model are compared in Table 1 with the exact result [29] (derived *after* the first numerical results were already published),

$$2\hat{\sigma}_{od} = \hat{\sigma}_{oo} = 1/\xi_d = \frac{1}{4}\sum_{n=0}^{\infty} \ln\left[\frac{1+w_n}{1-w_n}\right], \tag{36}$$

where $w_n = \left[\sqrt{2}\cosh\left((n+\frac{1}{2})\pi^2/2v\right)\right]^{-1}$ and the parameter v is defined by $v = \ln\left[\left((q^{1/2}+2)^{1/2} + (q^{1/2}-2)^{1/2}\right)/2\right]$. More precisely, $\hat{\sigma}_{od} = 1/\xi_d$, with $\xi_d(\beta_0)$ being the exactly calculated correlation length in the disordered phase at the transition point, is an exact relation, and also the bound $2\sigma_{od} \leq \sigma_{oo}$ was proved [52] for *all* $q \geq 5$. The opposite inequality could only be derived for $q > q_0$ (with $4 < q_0 < \infty$ being a sufficiently large constant), but by basic thermodynamic arguments it is commonly believed

TABLE 1. Comparison of analytical and numerical results for the order-disorder interface tension $2\hat{\sigma}_{od}$ in 2D q-state Potts models.

q	ξ_d	$2\hat{\sigma}_{od}$ (exact)	$2\hat{\sigma}_{od}$ (MC)	
7	48.095907	0.020792	0.0241(10)	Janke *et al.* [42]
			0.02348(38)	Rummukainen [43]
			0.0228(24)	Grossmann and Gupta [44]
8	23.878204	0.041879	0.045	Janke [31]
10	10.559519	0.094701	0.09781(75)	Berg and Neuhaus [41]
			0.10	Janke [31]
			0.0950(5)	Billoire *et al.* [46]
			0.09498(31)	at β_0, Janke [40]
			0.09434(40)	at $\beta_W(L)$, Janke [40]
15	4.180954	0.239179	0.263(9)	Gupta [47]
20	2.695502	0.370988	0.3714(13)	Billoire *et al.* [46]

that it actually also holds for all $q \geq 5$. So, strictly speaking, (36) is exact for all $q > q_0$, while for $q \leq q_0$ the r.h.s. of (36) is an exact upper bound on $2\hat{\sigma}_{od}$. Overall the numerical and analytical values in Table 1 are in good agreement, but noteworthy is the systematic trend of the numerical data obtained with the equal-peak-height method to overestimate the analytical values, which are actually exact *upper* bounds.

As a double-check, the formula (36) for the correlation length $\xi_d(\beta_0)$ has also been tested directly [55] by measuring the $k_y = 0$ projection $g(x)$ of the correlation function

$$G(i,j) = \langle \delta_{s_i s_j} - 1/q \rangle, \tag{37}$$

at β_0 in the disordered phase using a cluster estimator. By fitting with an ansatz appropriate for periodic boundary conditions, $g(x) = a\cosh((x - L/2)/\xi_d) + b\cosh(c(x - L/2)/\xi_d)$, we obtained for $q = 10$ estimates in the range $\xi_d(\beta_0) = 8.8(3)$ up to $10.2(9)$, depending on the lattice size (150×150 and 300×150) and fit range. These values are about $10\% - 20\%$ smaller than the exact value but (with a few exceptions) within the statistical errors still compatible. Similar analyses for $q = 15$ and 20 show the same qualitative trend [55]. Subsequently, by measuring the correlation length with a more refined and better adapted estimator, the cluster-diameter distribution function, the precision could be greatly improved and the exact values of $\xi_d(\beta_0)$ could be confirmed with an accuracy of about $1\% - 2\%$ for all considered values of q [56].

5. Summary

The main focus of this lecture was on the finite-size scaling behaviour of first-order phase transitions. For periodic boundary conditions, the generic behaviour of most quantities is an asymptotic power-law expansion in $1/V$ where V is the volume of the system. In addition exponentially small correction terms occur which, for the limited system sizes that can be simulated numerically, can be quite important in the data analyses. In practical applications it is often difficult to disentangle the two contributions. It is therefore gratifying that at least for some quantities improved estimators exist which are known to exhibit *only* exponentially small correction terms, and no power-law corrections at all.

Acknowledgments

This work was in part supported by the EC IHP network "EUROGRID: *Discrete Random Geometries: From Solid State Physics to Quantum Gravity* under contract No. HPRN-CT-1999-000161 and the German-Israel-Foundation under contract No. I-653-181.14/1999.

References

1. H.E. Stanley, *Introduction to Phase Transitions and Critical Phenomena* (Oxford University Press, Oxford, 1971).
2. N. Wilding, *Second-Order Phase Transitions*, this volume.
3. J.D. Gunton, M.S. Miguel, and P.S. Sahni, in *Phase Transitions and Critical Phenomena*, Vol. 8, eds. C. Domb and J.L. Lebowitz (Academic Press, New York, 1983).
4. K. Binder, Rep. Prog. Phys. **50** (1987) 783.
5. V. Privman (ed.), *Finite-Size Scaling and Numerical Simulations of Statistical Systems* (World Scientific, Singapore, 1990).
6. H.J. Herrmann, W. Janke, and F. Karsch (eds.), *Dynamics of First Order Phase Transitions* (World Scientific, Singapore, 1992).
7. J. Adler, A. Brandt, W. Janke, and S. Shmulyian, J. Phys. **A28** (1995) 5117.
8. K.M. Briggs, I.G. Enting, and A.J. Guttmann, J. Phys. **A27** (1994) 1503.
9. Y. Imry, Phys. Rev. **B21** (1980) 2042.
10. K. Binder, Z. Phys. **B43** (1981) 119.
11. M.E. Fisher and A.N. Berker, Phys. Rev. **B26** (1982) 2507.
12. V. Privman and M.E. Fisher, J. Stat. Phys. **33** (1983) 385.
13. K. Binder and D.P. Landau, Phys. Rev. **B30** (1984) 1477.
14. M.S.S. Challa, D.P. Landau, and K. Binder, Phys. Rev. **B34** (1986) 1841.
15. P. Peczak and D.P. Landau, Phys. Rev. **B39** (1989) 11932.
16. V. Privman and J. Rudnik, J. Stat. Phys. **60** (1990) 551.
17. For a review, see V. Privman in Ref. [5].
18. C. Borgs and R. Kotecký, J. Stat. Phys. **61** (1990) 79; Phys. Rev. Lett. **68** (1992) 1734.
19. C. Borgs, R. Kotecký, and S. Miracle-Solé, J. Stat. Phys. **62** (1991) 529.
20. C. Borgs and J.Z. Imbrie, J. Stat. Phys. **69** (1992) 487.
21. C. Borgs and R. Kotecký, J. Stat. Phys. **79** (1995) 43.

22. C. Borgs, R. Kotecký, and I. Medved', J. Stat. Phys. **109** (2002) 67.
23. M. Baig and R. Villanova, Phys. Rev. **B65** (2002) 094428.
24. For a general review of the Potts model, see e.g. F.Y. Wu, Rev. Mod. Phys. **54** (1982) 235; *ibid.* **55** (1983) 315 (*Erratum*).
25. R.J. Baxter, J. Phys. **C6** (1973) L445.
26. E. Buffenoir and S. Wallon, J. Phys. **A26** (1993) 3045.
27. A. Klümper, A. Schadschneider, and J. Zittartz, Z. Phys. **B76** (1989) 247.
28. A. Klümper, Int. J. Mod. Phys. **B4** (1990) 871.
29. C. Borgs and W. Janke, J. Phys. I (France) **2** (1992) 2011.
30. W. Janke and R. Villanova, Nucl. Phys. **B489** (1997) 679; and references therein.
31. W. Janke, Phys. Rev. **B47** (1993) 14757.
32. J. Lee and J.M. Kosterlitz, Phys. Rev. Lett. **65** (1990) 137; Phys. Rev. **B43** (1991) 3265.
33. W. Janke, unpublished notes.
34. C. Borgs and W. Janke, Phys. Rev. Lett. **68** (1992) 1738.
35. A.M. Ferrenberg and R.H. Swendsen, Phys. Rev. Lett. **61** (1988) 2635; *ibid.* **63** (1989) 1658 (*Erratum*).
36. W. Janke, *Histograms and All That*, this volume.
37. K. Binder, Phys. Rev. **A25** (1982) 1699.
38. B.A. Berg, Fields Inst. Comm. **26** (2000) 1; Comp. Phys. Comm. **104** (2002) 52.
39. W. Janke, Physica **A254** (1998) 164.
40. W. Janke, Nucl. Phys. **B** (Proc. Suppl.) **63A-C** (1998) 631.
41. B.A. Berg and T. Neuhaus, Phys. Rev. Lett. **68** (1992) 9.
42. W. Janke, B.A. Berg, and M. Katoot, Nucl. Phys. **B382** (1992) 649.
43. K. Rummukainen, Nucl. Phys. **B390** (1993) 621.
44. B. Grossmann and S. Gupta, Phys. Lett. **B319** (1993) 215.
45. A. Billoire, T. Neuhaus, and B.A. Berg, Nucl. Phys. **B396** (1993) 779.
46. A. Billoire, T. Neuhaus, and B.A. Berg, Nucl. Phys. **B413** (1994) 795.
47. S. Gupta, Phys. Lett. **B325** (1994) 418.
48. C. Chatelain, P.-E. Berche, B. Berche, and W. Janke, Comp. Phys. Comm. **147** (2002) 431.
49. B. Grossmann and M.L. Laursen, in Ref. [6], p. 375; and Nucl. Phys. **B408** (1993) 637; B. Grossmann, M.L. Laursen, T. Trappenberg, and U.-J. Wiese, Phys. Lett. **B293** (1992) 175.
50. B.A. Berg, U. Hansmann, and T. Neuhaus, Phys. Rev. **B47** (1993) 497; Z. Phys. **B90** (1993) 229.
51. W. Janke and T. Sauer, J. Stat. Phys. **78** (1995) 759.
52. J. de Coninck, A. Messager, S. Miracle-Solé, and J. Ruiz, J. Stat. Phys. **52** (1988) 45; R. Schonmann, J. Stat. Phys. **52** (1988) 61.
53. A. Messager, S. Miracle-Solé, J. Ruiz, and S. Shlosman, Commun. Math. Phys. **140** (1991) 275.
54. L. Laanait, Phys. Lett. **A124** (1987) 480.
55. W. Janke and S. Kappler, Phys. Lett. **A197** (1995) 227; Europhys. Lett. **31** (1995) 345;
56. W. Janke and S. Kappler, Phys. Rev. **E56** (1997) 1414.